

An experimental verification of numerical model on superheated steam drying of Belchatow lignite

M Zakrzewski¹, A Sciazko¹, Y Komatsu^{2,3}, T Akiyama³, A Hashimoto³,
S Kaneko³, S Kimijima^{4,3}, J S Szmyd¹, Y Kobayashi³

¹ Department of Fundamental Research in Energy Engineering, Faculty of Energy and Fuels, AGH University of Science and Technology, 30 Mickiewicza Avenue, 30-059 Krakow, Poland

² Division of Regional Environment Systems, Graduate School of Engineering and Science, Shibaura Institute of Technology, 307 Fukasaku, Minuma-ku, 337-8570 Saitama, Japan

³ Institute of Industrial Science, The University of Tokyo, 4-6-1 Komaba, Meguro-ku, 153-8505 Tokyo, Japan

⁴ Department of Machinery and Control Systems, College of Systems Engineering and Science, Shibaura Institute of Technology, 307 Fukasaku, Minuma-ku, 337-8570 Saitama, Japan

E-mail: zakrzews@agh.edu.pl

Abstract. Due to low production costs, lignite is an important component of energy mixes of countries in its possession. However, high moisture content undermines its applicability as fuel for power generation. Drying in superheated steam is a prospective method of upgrading quality of lignite. The study aimed to validate the drying model of lignite from Belchatow mine in Poland. The experimental investigation on superheated steam drying of lignite was previously conducted. Spheres of 10 mm in diameter were exposed to the drying medium at the temperature range of 110-170°C. The drying behaviour was described in the form of moisture content, drying rate and temperature profile curves against time. With the application of basic coal properties (e.g. density, water percentage, specific heat) as well as the mechanisms of heat and mass transfer in subsequent stages of the process, the numerical model of drying was constructed. It was tentatively verified with reference to experimental results both in terms of drying parameters and temperature. The model illustrated drying behaviour in the entire range of conditions. Nevertheless, further development of numerical model is desirable regarding accuracy of the process parameters.

1. Introduction

Lignite (known also as brown coal) plays an important role in economies of a number of countries, especially in Europe. The deposits of this fossil fuel are widely distributed and placed shallowly in the ground, what decrease production costs, resulting in cheap electricity generation [1]. However, due to limited coalification processes, its carbon content is lower than of bituminous coal. The share of burnable components in lignite is often balanced with moisture content, which undermines calorific value of this energy carrier.

Removal of water, intended to increase coal quality, should be performed with consideration of heat input rate required by the drying system and achieved increase in generated power. Regarding thermal efficiency, one of the prospective methods of water removal applicable for lignite is superheated steam drying.



Superheated steam as a drying medium has several features that enhance its applicability compared to commonly used hot air. Use of steam reduces the occurrence of spontaneous ignition and above a certain temperature ensures higher drying efficiency than hot air [2]. Nevertheless, the most crucial advantage relates to latent heat of water evaporation. The drying system working in self-heat recuperation configuration is capable of extracting the steam from the wet fuel entering the system and utilizing its latent and sensible heat to evaporate moisture from another batch of raw material [3,4]. In this way, the heat of phase change remains within the system, contributing to the growth of the thermal efficiency.

In order to design and construct a superheated steam drying (SSD) installation operating with a power generation unit, a detailed investigation of prospective fuel, including a numerical model of drying is required. This approach to drying process optimization has been widely applied in food industry. Tang et al. built a model of fixed bed dryer of brewers' spent grain operating on superheated steam [5]. Sa-Adchom et al. used finite difference method to predict changes of moisture content and center temperature in the slice of pork dried using the same medium [6]. SSD modelling has also been utilized also in power engineering, e.g. for combined heat and power operating on corn ethanol [7] and self-heat recuperative fluidized bed dryer of biomass, which allowed for 95% reduction in energy consumption compared to conventional systems [8]. The specificity of coal as a granular object in terms of drying was modelled by Chen et al. [9]. Kiriya et al. [10] prepared a single particle SSD model of Loy Yang lignite, using identical experimental methodology as in the present work.

In the present work an attempt was made to validate a numerical model elaborated using experimental results obtained in the previous study: investigation of the drying characteristics of Polish lignite excavated from the Belchatow deposit [11]. Simulating the drying behaviour with variable parameters aims to adjust the working conditions of a drying system under designing process.

2. Experimental methodology

2.1. Sample

The samples used in the experiment were sphere-shaped objects of 10 mm in diameter, weighing approximately 0.65 g in average. Precise preparation of the spheres was provided by rolling on a plate with several punctuated holes of diameter declining to demanded sample size.

In every sample, two thermocouples were placed to measure the interior temperatures. The tip of the first thermocouple reached the depth of 5 mm ("center" point), while the other was placed 2.5 mm under the surface ("midpoint").

2.2. Apparatus and procedure

During tests, a sample was placed in the test cylinder equipped with heaters and insulation to maintain uniform and stable temperature. The superheated steam was generated from distilled water. Degassed liquid was pumped to evaporator, turned to steam and superheated before entering the test cylinder through a baffle plate which uniformly dispersed the gas flow in the vessel. The water was fed at a flow rate of $8 \text{ cm}^3 \text{ min}^{-1}$.

The steam was kept under atmospheric pressure, while its temperature ranged between 110 and 170°C. The range was set in order to avoid water condensation at the bottom and coal volatilization at the top end. Below 180°C decomposition of lignite structure had not been observed [12], so the decline of weight might be attributed solely to water removal.

Two thermocouples mentioned in Subsection 2.1. and an infrared camera aimed at the sphere surface were used to measure the temperature profile in the process. The measurement of weight was realized by electronic balance, on which the rod with the sample was hanged. After steam drying has been completed, its flow was substituted with nitrogen to remove residual water. On the basis of the weight of sample after nitrogen drying two quantities, described in Subsection 2.3., were derived. The details of experimental methodology were described in the previous study [11].

2.3. Drying indicators

Moisture content X , is defined as the ratio of variable in time mass of water in coal to fixed mass of dry coal obtained after test. The formula is shown in equation (1):

$$X^i = \frac{m_w^i}{m_c} \quad (1)$$

Water percentage WP , is evaluated as share of water in the raw lignite sample. It is expressed as mass percentage as equation (2) presents:

$$WP^i = \frac{m_w^i}{m^0} \times 100 = \frac{m_w^i}{m_w^0 + m_c} \times 100 \quad (2)$$

3. Model

3.1. Physical model

The lignite sample was presumed to be a perfect sphere of isotropic properties. Therefore, a one-dimensional modelling along the radius might be applied. As presented in figure 1, the sphere was divided into 51 layers, of which first and last were half as thick as the others. The simulation of surface, midpoint and center temperature was performed on the 1st, 26th and 51st layer, respectively. The distribution of weight and temperature was assumed to be uniform within each layer.

The modelled sphere consisted of three phases: dry coal, free water (evaporating at 100°C) and bound water (evaporating above 100°C). The average water percentage of entire experimental set of spheres equaled 51.25%, what refers to moisture content of 1.05. The average density of particles, calculated using their initial weight, was 1205 kg m⁻³. The measured parameters allowed for the calculation of the density of dry coal as 1536 kg m⁻³. Taking into account the density of dry coal and assuming the density of water at 1000 kg m⁻³, the volumetric fractions of water and coal in the beginning of simulation were derived at 61.76% and 38.24%, respectively.

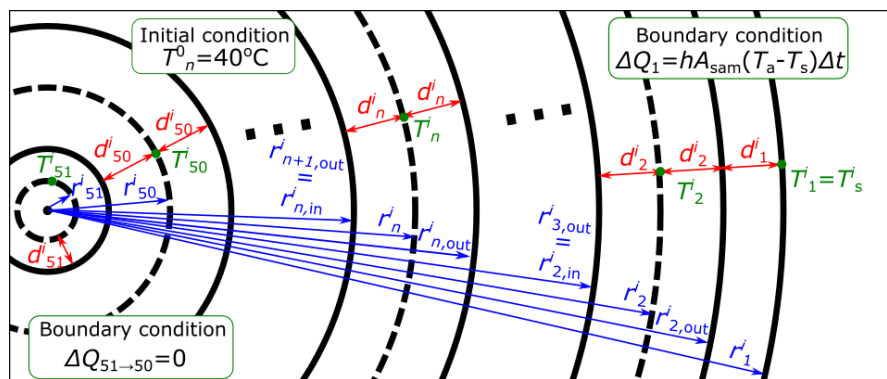


Figure 1. Simulation model of investigated lignite sphere.

3.2. Numerical model

3.2.1. General assumptions

The model applied in the present work was prepared with reference to previously published study on Loy Yang lignite from Australia [10]. Explicit method of computation was applied. No heat output was assumed from the central layer. The time step of the simulation was 0.001 s and the initial temperature was assumed at 40°C. The other parameters were taken to present physical and chemical properties of examined material. Although some of parameters presented in table 1 relate to different types of lignite, they were used due to lack of appropriate literature data on Belchatow lignite.

Table 1. Selected parameters used in simulation.

parameter	lignite type	remarks
specific heat	Belchatow	measured by the industrially standardized method (JIS K 0129)
thermal conductivity	Belchatow	calculated based on experimentation
equilibrium moisture content	Yallourn	temp. 100-100.3°C, taken from [10]
enthalpy change of bound water evaporation	Belchatow	temp. 100.3-170°C, derived experimentally
	Yallourn	taken from [10]

Relying on the experimental observations on Belchatow lignite included in the previous work of the authors [11], the numerical model was structurally divided into several consecutive parts. Each stage differed in terms of mechanisms governing heat and mass transfer between superheated steam and a dried object. In this Subsection, some insight in these mechanisms will be given.

Regardless of the drying period, the heat transfer within the sample is realized by means of conduction. The heat input to layer n can be expressed as in equation (3):

$$\Delta Q_n^{i+1} = (4\pi r_{n,out}^i) / (d_{n-1}^i / \lambda_{n-1}^i / r_{n-1}^i + d_n^i / \lambda_n^i / r_n^i) \cdot (T_{n-1}^i - T_n^i) \cdot \Delta t \quad (3)$$

3.2.2. Condensation

In the initial stage, when the temperature of coal remains below 100°C, the heat transferred to the sample is thought to be satisfied mostly by condensation of water on the surface.

$$\Delta Q_1^{i+1} = h_{\text{cond}} \cdot 4\pi (r_1^0)^2 \cdot (100 - T_s^i) \cdot \Delta t \quad (4)$$

At this time, entire heat is consumed in the layers on raising the temperature of water and coal.

$$\Delta Q_{\text{cons},n}^{i+1} = (c_c m_{c,n} + c_{w,n}^i m_{w,n}^i) \Delta T_n^i \quad (5)$$

3.2.3. Surface water evaporation

The surface temperature reaches then 100°C and is maintained at this level until the moisture on the surface evaporates. At this time, equation governing heat input to the sample is expressed as:

$$\Delta Q_1^{i+1} = h_{\text{exp,avg}} \cdot 4\pi (r_1^i)^2 \cdot (T_a - 100) \cdot \Delta t \quad (6)$$

Heat transfer coefficient was estimated on the basis of experiment using total mass of evaporated water in the constant drying rate period (equation (7)) and linearized as a function of the sample size.

$$h_{\text{exp,avg}} = -L / [4\pi (r_1^0)^2 \cdot (T_a - 100)] \cdot \frac{\Delta m_{w,\text{CDRP}}}{t_{\text{CDRP}}} \quad (7)$$

At this stage, the evaporation of surface water is provided with the difference between heat inputted to the sample (equation (6)) and its part transferred to the next layer (equation (3)).

3.2.4. Free water evaporation

After evaporation of surface water is done, the same means of heat input are assumed to be applied to the sample. The water in coal is regarded as free water when it evaporates at 100°C. When this mechanism of drying is applicable, heat is consumed only on evaporation.

$$\Delta Q_{\text{cons},n}^{i+1} = \Delta m_{\text{evap},n}^i L \quad (8)$$

Free water evaporation is inseparably connected with free water transfer between the layers. It was described as a function of moisture content in particular layers.

$$\Delta m_{\text{trans},n}^{i+1} = -D \rho_c 4\pi r_n^i r_{n+1}^i (X_n^i - X_{n+1}^i) / (d_n^i + d_{n+1}^i) \Delta t \quad (9)$$

3.2.5. Bound water evaporation

Oppositely to free water, bound water is kept tightly in the coal interior and turns to steam when the material temperature already exceed saturation temperature. Thus, when the temperature in particular layer started rising, it was assumed that no free water remained in that layer anymore. The heat transfer to the particle of surface temperature above 100°C is formulated as:

$$\Delta Q_1^{i+1} = h_{\text{exp,avg}} \cdot 4\pi(r_1^i)^2 \cdot (T_a - T_s^i) \cdot \Delta t \quad (10)$$

During bound water evaporation, the consumption of heat is divided between evaporation and temperature increase, according to the equation (11). At temperatures exceeding 100°C, heat required for water evaporation as well as equilibrium moisture content are functions of temperature. That makes mechanisms governing this part of simulation more complex than free water evaporation stage.

$$\Delta Q_{\text{cons},n}^{i+1} = [c_c m_{c,n} + c_{w,n}^i (m_{w,n}^i - \Delta m_{\text{evap},n}^i)] \Delta T_n^i + \Delta m_{\text{evap},n}^i \Delta H_n^i \quad (11)$$

According to the experimental observations, the decrease of moisture content below 0.6 for entire sample is accompanied with significant shrinkage phenomena. On that account, the linear shrinkage dependence was applied to modify the particle size during simulation. It was required for proper quantitative modelling of heat transfer phenomena in the drying process.

3.3. Initial validation

The initial water percentage within the experimental attempts ranged from 45 to 55% due to individualities of lignite. For that reason, the model was initially validated for two cases varying distinctly in terms of water percentage: 48.18% and 53.75%. The outcome is shown in figure 2.

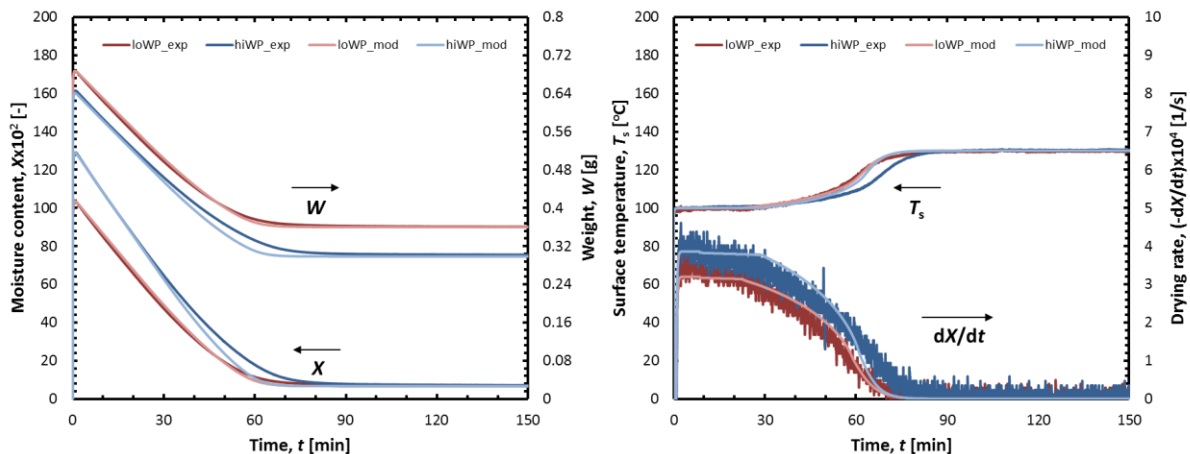


Figure 2. Comparison of experimental (exp) and numerical (mod) results for samples of 48.2% (loWP) and 53.7% (hiWP) water percentage dried in 130°C.

Good consistency of experimental and numerical results was achieved. The particles with larger amount of water exhibited lower weight at the beginning and conclusion of the process. That fact arises from lower share of dry coal part, which is characterized with higher density than water.

The model exceeded experiment in terms of moisture content after condensation period only for lower moisture content instance. In case of high moisture content case, the simulated level of the drying rate turned out to be higher than measured one. Hence, the weight decrease became more rapid in the model. What is more, the temperature growth was also delayed in this instance. When around 55 minutes have passed, the weight gap between empirical and numerical results was at the highest level and right after the simulated drying rate fell below experimental data, it started to close down.

Note that weight charts of different samples normally do not tend to the same final value, while the moisture content charts do. After a certain period of drying, vapour partial pressure of water in lignite is equal to the partial pressure of water in surrounding gas (in case of steam drying it is equal to total steam pressure). This state is known as equilibrium moisture content and no further reduction of water amount occurs afterwards. Two objects varying in attributes such as initial water percentage, resulted from different structures of coal, are not supposed to attain equal level of moisture content by the end of the process. The properties of various samples, though, are similar enough to reach very close values of final moisture when dried in identical thermal conditions. Thus, the equilibrium moisture content equation is here described as a function of temperature only.

4. Results

4.1. Comparison of empirical and numerical results

The outcome of the computation was compared with experimental data as shown on figure 3. The simulation was conducted for averaged parameters indicated in Subsection 3.1. On the other hand, the experimental cases varied in properties, what is exhibited, for instance, by differences in moisture content curves. Midpoint temperatures were deliberately omitted for the sake of figure's clarity.

Concluding from the charts, high temperature entailed the elevated speed of drying. For that reason, water from lignite was discarded sooner and sample reached thermal equilibrium with steam, reducing the time required for the completion of the process.

The rate of temperature increase was more gradual for experimental results and it occurred sooner than simulation predicted. Furthermore, the distinction between surface and center temperature, explicit for all calculations, was maintained for experiments A and B only. The model adapted in this study assumed increase of temperature only after the complete removal of free water in particular layer. Because of lignite irregular structure and deformations occurring during drying, the phase border between free and bound water might move with various pace within different cross-sections, making the temperature profile inconsistent with the calculated prediction.

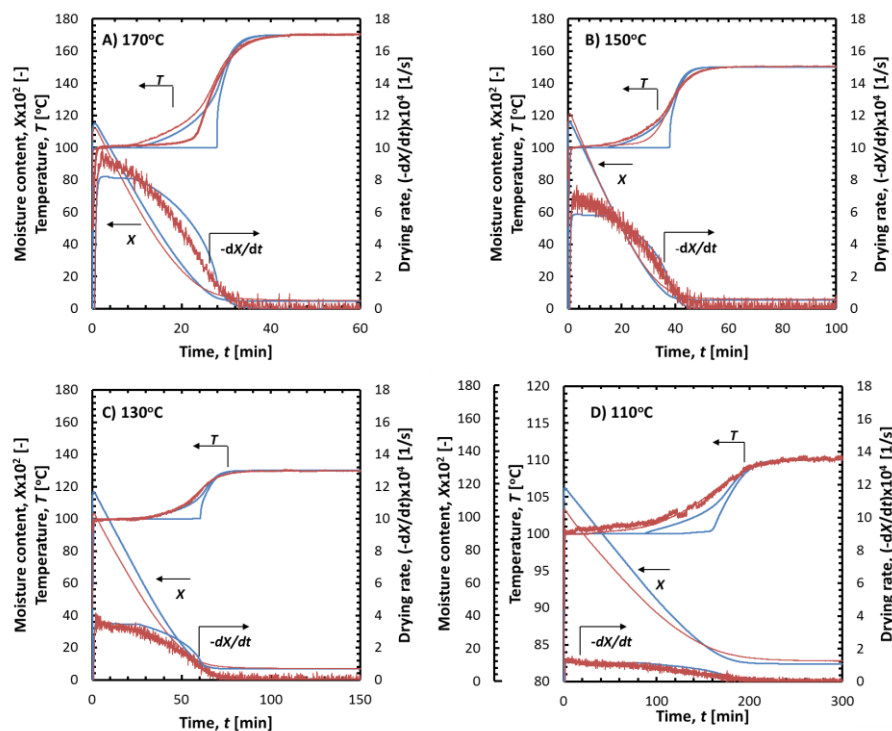


Figure 3. Simulated values (blue) of moisture content, drying rate and temperatures compared to experimental results (red) at test temperatures of A)170°C, B)150°C, C)130°C and D)110°C.

4.2. Prediction of temperature dependence on drying performance

The simulation of drying was conducted for in the steam temperature range 110 – 170°C for average lignite properties introduced in Subsection 3.1. Selected parameters are gathered in table 2. The predicted time of drying t_{dry} is rapidly increasing with the temperature decrease down to 100°C. Reduction from 120 to 110°C results in extending the process by 96%. The highest level of drying rate $(dX/dt)_{max}$ was observed for the highest temperature. The period, when dewatering is the most intense t_{CDRP} , was simulated to last from 2% (170°C) to 11% (110°C) of total drying time. Total removal of free water, signalized by center temperature increase over 100°C, t_{free} , occurs around 1/2 of process conducted in higher temperatures and reduces to 1/3 near saturation temperature. The highest temperature gradient between surface and center $\Delta T_{1,51,max}$ was simulated at 35.3°C.

Table 2. Drying parameters prediction.

T [°C]	t_{dry} [min]	t_{CDRP} [min]	$(dX/dt)_{max}$ [s ⁻¹]	t_{free} [min]	$\Delta T_{1,51,max}$ [°C]
170	62.0	1.4	8.19	26.4	35.3
160	69.2	2.0	7.02	29.6	29.8
150	79.6	2.9	5.85	34.5	24.4
140	95.5	4.1	4.68	39.5	18.9
130	122.4	6.3	3.51	49.2	13.4
120	177.5	10.6	2.34	63.9	8.0
110	348.6	38.2	1.17	109.7	3.1

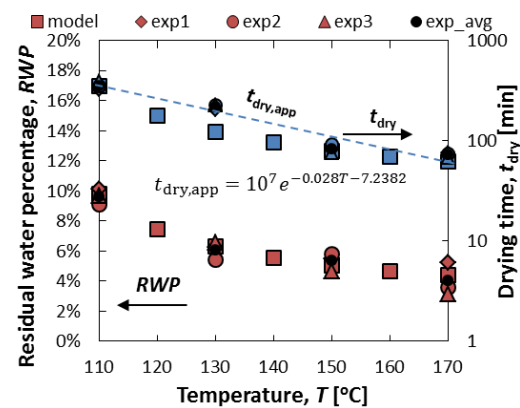


Figure 4. Residual water and drying time.

In figure 4, a comparison of simulated (square marker) and empirical quantities was shown. The simulated and empirical results for residual water agree well as the equilibrium moisture equation was elaborated on the basis of the experiment (see table 1). In case of drying time, an approximation curve, elaborated in the previous study [11], was included for comparison. Table 3 presents experimental values of drying time t_{exp} altogether with their standard deviations ($s(t_{exp})$). Moreover, the root-mean-square error calculated for experimental values and both approximation $R(t_{dry,app})$ and model $R(t_{dry})$, respectively. The outcome of empirically-based approximation, similarly to actual results, exhibits increasing consistency when the temperature rises. On the other hand, model provides greater accuracy for all cases but 130°C, which is significantly underestimated. Therefore, further effort needs to be put to modify the equation type for approximation as well as the numerical model of simulation.

Table 3. Accuracy of drying time prediction.

T [°C]	t_{exp} [min]			$s(t_{exp})$ [min]	$t_{dry,app}$ [min]	$R(t_{dry,app})$ [min]	t_{dry} [min]	$R(t_{dry})$ [min]
170	76.0	73.1	68.0	3.3	61.6	11.3	62.0	8.1
150	81.1	92.7	74.8	7.4	107.8	25.9	79.6	10.9
130	200.0	226.5	224.2	12.0	188.7	30.7	122.4	95.2
110	316.8	346.0	394.0	31.8	330.3	38.7	348.6	32.0

5. Conclusions

This work describes an attempt to verify the numerical model simulating superheated steam drying of 10 mm sphere made of the Belchatow lignite. Draft analysis of the modelling accuracy as well as temperature dependence on obtained results was performed. Further optimization of the calculations is required and should be related to elaborating input parameters strictly for analysed type of lignite. Numerical studies are indispensable component of the designing process of an actual dryer.

Nomenclature

Symbols:

c – specific heat [$\text{J kg}^{-1} \text{ } ^\circ\text{C}^{-1}$]
 d – half of layer's thickness [m]
 D – apparent transfer coefficient of free water [$\text{m}^2 \text{ s}^{-1}$]
 e – emissivity [-]
 h – heat transfer coefficient [$\text{W m}^{-2} \text{ } ^\circ\text{C}^{-1}$]
 ΔH – enthalpy change of bound water evaporation [J kg^{-1}]
 λ – thermal conductivity [$\text{W m}^{-1} \text{ } ^\circ\text{C}^{-1}$]
 L – latent heat of free water [J kg^{-1}]
 m – mass [kg]
 Δm – change of mass [kg]
 ΔQ – heat input/consumption [J]
 r – radius [m]
 R – root-mean-square error
 ρ – density [kg m^{-3}]
 σ – Stefan's constant [$\text{W m}^{-2} \text{ K}^{-4}$]
 t – time [s]
 Δt – time step [s]
 T – temperature [$^\circ\text{C}$]
 ΔT – change of temperature [$^\circ\text{C}$]

Sub- and superscripts:

a – superheated steam
app – approximated
avg – average
b – boundary
c – dry coal
CDRP – constant drying rate period
cond – condensation
cons – consumption
conv – convective
dry – drying
evap – evaporated water
exp – experimental
free – referring to free water
i – time instance
n – referring to *n*-th layer
s – surface
rad – radiative
trans – water transfer
w – water

Acknowledgements

The present study was financially support by the Japan Coal Energy Center (JCOAL) and the Polish National Centre for Research and Development (NCBR Project: I_POL-JAP, SSD-4-LRC).

References

- [1] Patrycy A 2011 *Górnictwo i Geoinżynieria (AGH J. Min. Geoengin.)* **35** 249–60
- [2] Yoshida T and Hyodo T 1970 *Ind. Eng. Chem. Process Des. Dev.* **97** 207–14
- [3] Fushimi C, Kansha Y, Aziz M, Mochidzuki K, Kaneko S, Tsutsumi A, Matsumoto K, Yokohama K, Kosaka K, Kawamoto N, Oura K, Yamaguchi Y and Kinoshita M 2010 *Dry. Technol.* **29** 105–10
- [4] Mujumdar A S 2006 Superheated steam drying *Handbook of Industrial Drying* ed Mujumdar A S (Boca Raton: CRC Press) 439–52
- [5] Tang Z, Cenkowski S and Muir W E 2004 *Biosyst. Eng.* **87** 67–77
- [6] Sa-Adchom P, Swasdisevi T, Nathakaranakule A and Soponronnarit S 2011 *J. Food Eng.* **104** 499–507
- [7] Morey R V, Zheng H, Kaliyan N and Pham M V. 2014 *Biosyst. Eng.* **119** 80–8
- [8] Liu Y, Kansha Y, Ishizuka M, Fu Q and Tsutsumi A 2015 *Fuel Process. Technol.* **136** 79–86
- [9] Chen Z, Wu W and Agarwal P K 2000 *Fuel* **79** 961–73
- [10] Kiriyama T, Sasaki H, Hashimoto A, Kaneko S and Maeda M 2013 *Mater. Trans.* **54** 1725–34
- [11] Komatsu Y, Sciazko A, Zakrzewski M, Kimijima S, Hashimoto A, Kaneko S and Szmyd J S 2015 *Fuel Process. Technol.* **131** 356–69
- [12] Umar D F, Usui H and Daulay B 2005 *Coal Prep.* **25** 313–22